Published in final edited form as:
Exp Neurol. 2008 March ; 210(1): 14–29.

Autologous transplants of Adipose-Derived Adult Stromal (ADAS) afford dopaminergic neuroprotection in a model of Parkinson's disease

Melissa K. McCoy[1,*], **Terina N. Martinez**[1,*], **Kelly A. Ruhn**[1], **Philip C. Wrage**[1], **Edward W. Keefer**[2], **Barry R. Botterman**[3], **Keith E. Tansey**[4], and **Malú G. Tansey**[1]

1 *Department of Physiology, The University of Texas Southwestern Medical Center*

2 *Department of Plastic Surgery, The University of Texas Southwestern Medical Center*

3 *Department of Cell Biology, The University of Texas Southwestern Medical Center*

4 *Department of Neurology, The University of Texas Southwestern Medical Center*

Abstract

Adult adipose contains stromal progenitor cells with neurogenic potential. However, the stability of neuronal phenotypes adopted by Adipose-Derived Adult Stromal (ADAS) cells and whether terminal neuronal differentiation is required for their consideration as alternatives in cell replacement strategies to treat neurological disorders is largely unknown. We investigated whether *in vitro* neural induction of ADAS cells determined their ability to neuroprotect or restore function in a lesioned dopaminergic pathway. *In vitro*-expanded naïve or differentiated ADAS cells were autologously transplanted into substantia nigra 1-week after an intrastriatal 6-hydroxydopamine injection. Neurochemical and behavioral measures demonstrated neuroprotective effects of both ADAS grafts against 6-hydroxydopamine-induced dopaminergic neuron death, suggesting that pre-transplantation differentiation of the cells does not determine their ability to survive or neuroprotect *in vivo*. Therefore, we investigated whether equivalent protection by naïve and neurally-induced ADAS grafts resulted from robust *in situ* differentiation of both graft types into dopaminergic fates. Immunohistological analyses revealed that ADAS cells did not adopt dopaminergic cell fates *in situ*, consistent with the limited ability of these cells to undergo terminal differentiation into electrically active neurons *in vitro*. Moreover, re-exposure of neurally-differentiated ADAS cells to serum-containing medium *in vitro* confirmed ADAS cell phenotypic instability (plasticity). Lastly, given that gene expression analyses of *in vitro*-expanded ADAS cells revealed that both naïve and differentiated ADAS cells express potent dopaminergic survival factors, ADAS transplants may have exerted neuroprotective effects by production of trophic factors at the lesion site. ADAS cells may be ideal for *ex vivo* gene transfer therapies in Parkinson's disease treatment.

Corresponding author: Malú G. Tansey, PhD, Assistant Professor of Physiology, The UT Southwestern Medical Center, 5323 Harry Hines Blvd., Dallas, TX 75390, malu.tansey@utsouthwestern.edu.
Melissa.mccoy@utsouthwestern.edu
Terina.martinez@utsouthwestern.edu
Kelly.ruhn@utsouthwestern.edu
Philip.Wrage@utsouthwestern.edu
Edward.keefer@utsouthwestern.edu
Barry.botterman@utsouthwestern.edu
Keith.tansey@utsouthwestern.edu
Malu.tansey@utsouthwestern.edu
*equal contribution

Keywords

stromal adipose; neural differentiation; autologous transplantation; dopaminergic; neuroprotection; Parkinson's disease; 6-hydroxydopamine; tyrosine hydroxylase

INTRODUCTION

Because central nervous system tissue has limited capacity for intrinsic repair after injury, cell replacement strategies represent an attractive approach for neurorestorative medicine (Weissman 2000). Endogenous neural stem cells within certain regions of the adult brain can be proliferated *in vitro* (Gage, Ray et al. 1995; Gage 2000). However, regulation of their growth and proliferation potential *in vivo* remains a major problem (Hermann, Gerlach et al. 2004; Belmadani, Tran et al. 2006; Conti, Reitano et al. 2006; Miller 2006). Similarly, widespread use of fetal tissue or embryonic stem cells in cell replacement therapies has been limited by histocompatibility issues, availability, and ethical concerns prompting the search for alternative cell sources (Frankel 2000; Sonntag and Sanchez-Pernaute 2006). Of particular interest are other adult tissues with progenitor populations that could be easily harvested, expanded, and used in autologous transplantation strategies to protect vulnerable neuronal populations and/or to accelerate repair after neural injury or neurodegeneration without the need for immunosuppression. Subpopulations of cells residing within adult liver (Alison and Sarraf 1998), intestine (Potten 1998), skin/hair-follicles (Fernandes, McKenzie et al. 2004; Amoh, Li et al. 2005), and bone marrow (Jiang, Jahagirdar et al. 2002; Jiang, Vaessen et al. 2002) express neuroectodermal or neural crest cell markers *in vitro* and/or *in vivo*. Similarly, adult bone marrow-derived mesodermal stromal cells (MSC) display neurogenic properties (Woodbury, Schwarz et al. 2000; Jiang, Jahagirdar et al. 2002; Jiang, Vaessen et al. 2002; Woodbury, Reynolds et al. 2002; Dezawa, Kanno et al. 2004; Hermann, Gastl et al. 2004; Bonilla, Silva et al. 2005; Bossolasco, Cova et al. 2005; Hermann, Maisel et al. 2006) including the ability to fire action potentials and respond to neurotransmitters, including GABA, glycine, and glutamate (Wislet-Gendebien, Hans et al. 2005).

In recent years, adult adipose was shown by several laboratories (reviewed in (Schaffler and Buchler 2007) to be a source of multipotent cells from which to derive progenitors such as chondrocytes, adipocytes, osteoblasts, and myocytes for tissue engineering and repair of mesodermal or mesenchymal-derived tissues (Zuk, Zhu et al. 2001; Zuk, Zhu et al. 2002; Tholpady, Katz et al. 2003) while others reported adipose may also have sub-populations of cells with neurogenic potential *in vitro* (Safford, Hicok et al. 2002; Ashjian, Elbarbary et al. 2003; Kang, Putnam et al. 2004; Safford, Safford et al. 2004; Fujimura, Ogawa et al. 2005; Ning, Lin et al. 2006). The term Adipose-Derived Adult Stem (ADAS) cells was the original term used to refer to these cells on the basis of their potential for multi-lineage specification (Safford, Hicok et al. 2002). However, strict criteria for 'stemness' has not been met conclusively (Weissman, Anderson et al. 2001; Easterday, Dougherty et al. 2003; Lakshmipathy and Verfaillie 2005). Therefore, the preferred term for these cells, and the one which we use in our study, is Adipose-Derived Adult Stromal (ADAS) cells (Safford, Safford et al. 2004). Despite significant progress in characterization of cell surface markers for ADAS cells (Guilak, Lott et al. 2006; Izadpanah, Trygg et al. 2006), therapeutic benefit derived from transplantation of ADAS cells has yet to be demonstrated in animal models of neurodegeneration.

The primary goal of these studies was to investigate the extent to which autologous grafts of naïve or neurally-induced rat ADAS cells protect, repair, or restore function of the nigrostriatal pathway in a neurotoxin model of Parkinson's disease (PD). Neurochemical and behavioral measures confirmed the neuroprotective effects of both kinds of autologous ADAS cell grafts

against 6-hydroxydopamine (6-OHDA)-induced dopaminergic neuron death. On the basis of neurohistological, cell biological, electrophysiological, and gene expression studies, we concluded that the mechanism by which ADAS cell grafts contributed to improved nigrostriatal function does not involve stable differentiation of ADAS cells into functional dopaminergic neurons. Our findings suggest that modulation of the oxidative stress-induced neuroinflammatory environment in the lesioned substantia nigra and/or ADAS-derived production of growth factors known to promote dopaminergic survival and neuroprotection at the lesion site may have contributed to the therapeutic effects of ADAS cell transplants.

Materials and Methods

Animals

All animal procedures were approved by the Institutional Care and Use Committee at UT Southwestern. Animals were housed in a climate controlled facility staffed with certified veterinarians.

Survival surgeries to harvest adipose tissue

For survival surgeries, adult female Sprague-Dawley rats (200–225 g) were anesthetized with 2% halothane and a 0.75cm^2 portion of the interscapular fat pad was excised during a survival surgery when a unilateral striatal 6-hydroxydopamine injection was performed. The adipose tissue was rinsed in cold sterile PBS (Ca/Mg Free, Invitrogen Inc., Carlsbad, CA) and incubated for 1 hr in Dulbecco's Modified Eagle's Medium (DMEM, Invitrogen) supplemented with 10% fetal bovine serum (FBS, Atlanta Biologicals, Lawrenceville, GA) and antibiotic/antimycotic (Invitrogen) prior to dissociation. Fat pads were mechanically triturated then enzymatically digested in collagenase (Invitrogen) for 1 hr at 37 degrees C followed by mechanical dissociation to yield a stromal cell suspension which was collected by centrifugation (x1000g). The cell pellet was resuspended in DMEM supplemented with 10% FBS (D10 medium) and plated (Day 0, P0) onto 35mm tissue culture-treated dishes.

Expansion and Neural induction of ADAS cells for Immunocytochemical Analyses

Non-adherent cells in P0 cultures were removed 24h post-plating in order to expand the small number of adherent stromal cells (< 10% of total cells plated) by serial passage. Media was replenished every 3 days and cultures were serially passaged at 75% confluence at a 1:4 ratio. Differentiation of cultures (P2 to P4) consisted of pre-induction of cultures plated in D10 with 10ng/ml EGF (R&D Systems, Minneapolis, MN) and 20ng/ml FGF-2 (R&D) for 2 to 3 days prior to a 4-day exposure to either of the following: Neural Differentiation Medium [NDM: D10, 120 uM indomethacin (Sigma-Aldrich, St. Louis, MO), 3ug/mL insulin (Sigma-Aldrich), 300 uM isobutyl-methylxanthine (Sigma-Aldrich)] or N2-supplemented/VPA [N2/VPA: DMEM, N2 supplement (Invitrogen), 0.5mM valproic acid (Sigma-Aldrich)] to induce gradual neuronal differentiation and outgrowth of processes. Alternatively, differentiation was achieved by pre-induction of cultures grown in D10 by exposure to 10ng/ml EGF + 20 ng/ml FGF-2 (E/F) in NS-A Proliferation medium (Stem Cell Technologies, Vancouver, BC) for 3 days followed by 4-day differentiation in NS-A Differentiation supplement (Stem Cell Technologies). Where indicated, specific differentiation factors [1uM all-trans retinoic acid, 1–10 uM forskolin, 10–50 ng/ml Glial cell-derived neurotrophic factor (GDNF) or 10ng/ml Brain-Derived Neurotrophic Factor (BDNF)] were used to investigate their effects on process outgrowth of ADAS cells.

Immunocytochemical detection of neural and glial markers

Cells in culture were fixed in 4% paraformaldehyde (PFA) for 20 minutes prior to blocking/permeabilization for immunocytochemistry with antibodies to Nestin (BD Pharmingen, San

Diego, CA), vimentin (Chemicon, Temecula, CA), Fibronectin (Sigma-Aldrich), Neuron Specific Enolase (Polysciences Inc., Warrington, PA), VE cadherin (Santa Cruz Biotechnology, Santa Cruz, CA), Neuro D (Santa Cruz), Tubulin beta III/Tuj1 (Covance, Princeton, NJ), MAP2b (Chemicon), NeuN (Chemicon), Gamma-Amino Butyric Acid or GABA (Chemicon), TrkB (Chemicon), Choline Acetyl Transferase or ChAT (Chemicon), tyrosine hydroxylase or TH (Chemicon), smooth muscle actin or SMA (Sigma-Aldrich), CD11b or OX-42 (Santa Cruz), Glial Fibrillary Acidic Protein or GFAP (Chemicon), oligodendrocyte marker O4 (R&D), the Schwann cell marker S100β (Sigma-Aldrich), low-affinity neurotrophic factor receptor p75NTR (Chemicon), and myelin basic protein or MBP (Chemicon). Detection of desired antigens was achieved through use of the appropriate secondary antibody conjugated to Alexa-488 or Alexa-594 diluted 1:1000 (Invitrogen). IgG or IgM control sera were used at the same concentration as the corresponding primary antibodies to establish the specificity of staining. Total cell nuclei were visualized with the nuclear dye Hoechst 33258 (bis-benzimide). A CoolSnap ES (monochrome) camera mounted on an upright Olympus BX61 or an inverted Olympus CK40 fluorescence scope and MetaMorph software were used for image capture and analyses.

Phenotypic stability studies of ADAS cells in vitro

ADAS cells were fixed for immunocytochemical analysis at each step along the treatment regimen which began in D10, followed by 2 days of EGF/FGF-2, followed by 4 or 7 days of NDM or N2/VPA, followed by 1 or 2 days of D10. A survey of immunoreactivity for each protein marker was performed using immunofluorescence analysis of each treatment condition at high (40X objective) and low (10X objective) magnification. Scores between 1 and 4 were given based on fluorescence intensity and fraction of total cells expressing that particular marker according to the following scale: 4 = robust immunoreactivity in many (> 50 %) of the cells, 3 = strong staining in approximately 50% of the cells, 2 = detectable staining in less than 50% of the cells, 1 = detectable staining in a small fraction (< 10%) of the cells, 0 = no detectable immunoreactivity.

Survival surgeries for fat pad harvest and intrastriatal 6-OHDA injection

6-hydroxydopamine (6-OHDA) lesions were performed as described previously (McCoy, Martinez et al. 2006). Briefly, young adult female Harlan Sprague Dawley SASCO rats (200–225 g) (n= 4 or 5 per group) were anesthetized with halothane (2%) and placed in a stereotaxic head-holder frame with the incisor bar set at −2.5 mm as per the rat stereotaxic atlas (Paxinos 1998). Burr holes were drilled at stereotaxic coordinates (AP): −1.2 mm from bregma, mediolateral in right hemisphere (ML): −3.9 mm; and dorsoventral (DV): −5 mm below surface of dura) (Paxinos, Watson et al. 1985) to perform unilateral injection of 20 μg 6-OHDA (4 μL of 5 μg/μL in ascorbic acid, Sigma-Aldrich) at a rate of 1 μL/min into the striatum with a 5 uL Hamilton micro syringe and a 30 gauge needle. Fat pads from the interscapular region were also harvested from all experimental animals at this time (including rats that were to receive a sham-transplant) for *in vitro* expansion of ADAS to passage 2 (P2) as described above. This unilateral intrastriatal 6-OHDA injection was chosen to induce a moderate retrograde lesion in the nigrostriatal pathway resulting in the loss of approximately 65–70% of TH-positive somata in the SNpc three weeks after the lesion (Kirik, Rosenblad et al. 1998; McCoy, Martinez et al. 2006). Seven days after 6-OHDA lesion, drug-induced rotational behavior testing was conducted to establish a baseline for locomotor behavior just prior to cell transplantation.

Rotational behavior analyses

The extent of the retrograde nigrostriatal lesion was physiologically characterized using amphetamine-induced rotational behavior testing (Ungerstedt and Arbuthnott 1970). Animals

received 2.5 mg/kg D-amphetamine (Sigma, St. Louis) i.p. and were subsequently placed in a glass cylinder (diameter 24.5 cm) to monitor rotational asymmetry for 20 min. Drug-induced rotational behavior was measured prior to the transplant (one week post 6-OHDA injection) as well as at 1, 2, and 3 weeks post-transplantation to assess effects of the ADAS grafts. Rotation towards the lesion (ipsilateral) was scored as positive and net rotational asymmetry score was expressed as full body turns.

Stereotaxic transplantation of MTR-labeled ADAS grafts

One week after intrastriatal 6-OHDA or saline injection and fat pad harvesting, cell transplants were performed. On the day of transplantation, passage 2 ADAS were labeled with 95–100% efficiency with the fixable mitochondrial dye CMH_2Xros MitoTracker Red (MTR) which fluoresces in a membrane potential-dependent manner (Poot, Zhang et al. 1996). After MTR loading, the cells were rinsed and resuspended at a density of 4×10^6 per mL in order to deliver approximately 40,000 cells (4 ul of 10,000/ul) per animal into the substantia nigra in the hemisphere ipsilateral to the 6-OHDA-or saline-injected striatum via stereotaxic injection using a 10ul Hamilton microsyringe with a 30 gauge needle at rate of 1uL/min via automated infusion pump using the following stereotaxic coordinates: AP −5.3mm, ML −2.4mm, DV −6.0mm below surface of dura; incisor bar at −2.5 mm. Lesioned rats received E/F treated naïve ADAS (n = 5), NDM differentiated ADAS (n = 5), or saline (n = 4). A control (unlesioned) group of rats (n = 4) was also included.

Perfusion and tissue processing for histology

Animals were deeply anesthetized with Euthasol and intracardially perfused as described previously (Kirik, Rosenblad et al. 1998; McCoy, Martinez et al. 2006) four weeks after autologous transplantation (i.e. five weeks post lesion). Brains were then removed from the skull and post-fixed for 24 h in the same PFA solution, cryoprotected in 20% sucrose in PBS for 18–24 hr, and frozen by embedding in Tissue-tek cooled by a dry-ice/isopentane solution. Coronal sections (30 μm-thickness) were cut through the striatum and substantia nigra pars compacta (SNpc) on a Leica CM1850 cryostat and mounted on glass slides (SuperFrost Plus, Fisher) for immunohistological analyses and stereological estimate of DA neuron number in SNpc.

Immunohistochemistry of brain sections

Processing of brain sections was done as described previously (Kirik, Rosenblad et al. 1998; McCoy, Martinez et al. 2006). IgG or IgM sera were used at the same concentration as the corresponding primary antibodies to confirm the specificity of staining.

Stereological Nigral DA neuron counts

StereoInvestigator analyses software (Micro Bright Field Inc., Williston, VT) was used to perform unbiased stereological counts of TH-immunoreactive (TH-IR) cell bodies in the SNpc using the optical fractionator method (West, Slomianka et al. 1991) as described previously (Kirik, Rosenblad et al. 1998; McCoy, Martinez et al. 2006). The boundary of SNpc was outlined under magnification of the 4X objective as defined according to previous anatomical demarcation in the rat (German and Manaye 1993). For analysis, the treatment of the various brain sections was blinded to the observer. Cells were counted with a 60X oil immersion objective (1.3 NA) using an Olympus BX61 microscope. Serial sections through the extent of SNpc (from AP:−3.3mm to −5.3mm behind bregma) were cut on a Leica cryostat and placed 4 per slide (cut thickness of 30μm and mounted thickness of 22 μm) for systematic analysis of randomly placed counting frames (size 50 × 50 μm) on a counting grid (size of 160 μm × 120 μm) and sampled using an 18μm optical dissector with 2 μm upper and lower guard zones. Every other slide was stained for TH/NeuN and the intervening slide was analyzed for

MitoTracker Red fluorescence. A dopaminergic neuron was defined as a TH immunoreactive cell body with a clearly visible TH-negative nucleus. An ADAS cell was defined as a MTR-positive cell. The reason for assessing *in vivo* differentiation of ADAS post transplantation was to determine if MitoTracker Red-positive cells also co-expressed a particular cell fate marker (i.e. tyrosine hydroxylase for differentiation into dopaminergic cell fate).

Quantification of striatal TH-fiber density

Striatal optical density (OD) of TH immunostaining, determined by digital image analysis on Image Pro Plus 5.1, was used as an index of striatal density of TH innervation; densitometric measurements have been shown to provide valid relative indices of extent of fiber innervation on the same brain section of an animal receiving a unilateral 6-OHDA lesion (Burke, Cadet et al. 1990). ODs were measured to estimate dopaminergic fiber innervation into the striatum. The density readings of TH-immunoreactivity in the striatum on both hemispheres of each animal were corrected for nonspecific background density, as measured on sections stained with non-immune IgG serum. Striatal images taken under a 4x objective converted to gray scale were then delineated and the intensity of staining was thus assessed for the entire striatal region (boundaries according to the rat stereotaxic atlas) of the four sections sampled for the ipsilateral and for the contralateral striatum, subsequently averaged for each animal to obtain average optical density (AOD). The data are expressed as percent fiber density of the ipsilateral (experimental) side relative to the contralateral (control) side. Values expressed are group means ± S.D. Values were compared by one-way ANOVA followed by Tukey-Kramer HSD post-hoc test. Groups with different letters are significantly different at $p<0.05$.

Quantification of microglial burden

To estimate the microglial burden in the SNpc, optical density of the OX-42 immunoreactivity in the SNpc was obtained by digital image analysis using the Image-Pro Plus 5.1. The density readings were corrected for nonspecific background density as measured on sections stained with non-immune IgG serum. SNpc images taken under a 4x objective converted to gray scale were then delineated and the intensity of staining was thus assessed for the entire SNpc region (boundaries according to the rat stereotaxic atlas) of the six sections sampled throughout the extent of SNpc, subsequently averaged for each animal. The data was expressed as integrated optical density (IOD). All data are expressed as mean ± S.E.M. Inter-group differences between the various dependent variables were assessed using one-way ANOVA, followed by the Tukey's post hoc multiple comparisons test. Data obtained were analyzed by GraphPad statistic software; $p < 0.05$ were considered significant.

Assessment of Phenotypic Stability of ADAS cells in vitro

Cells were proliferated in base media (D10) to passage 2 or 3 followed by supplementation with 10 ng/mL EGF and 20 ng/mL FGF-2 (E/F) for 2–3 days. Differentiation was induced by mitogen withdrawal and exposure to the indicated medium formulations (NDM or N2/VPA). Following a period of 7 days of differentiation, the cells were returned to D10 medium for 24 or 48 hrs prior to harvesting for marker analyses by immunocytochemistry. A qualitative survey of immunoreactivity for each protein marker was performed at high (40X) and low (10X) magnification and scores between 1 and 4 were given based on fluorescence intensity and fraction of total cells expressing that particular marker according to the following scale: 4 = intense immunoreactivity in many (> 50 %) of the cells, 3 = strong staining in ~ 50% of the cells, 2 = detectable staining in less than 50% of the cells, 1 = detectable staining in a small fraction (< 10%) of the cells, 0 = no detectable immunoreactivity.

Real-time Quantitative PCR

Quantitative real-time PCR was performed as previously described (Kurrasch, Huang et al. 2004). Briefly, total RNA was isolated with RNAStat60 (Tel-Test Inc., Friendswood, TX) from cultured cells or rat tissues, treated with DNase I, and reverse transcribed using Superscript II RNase H- reverse transcriptase (Invitrogen). Quantitative real-time PCR was performed using an ABI Prism 7000 Detection System (Applied Biosystems, Foster City, CA). Each reaction was performed in 384-well plate format in a volume of 10 ul that contained 3.5 ng cDNA, 7ul SYBR green PCR Master Mix, and 200 nM of each PCR primer. All reactions were performed in duplicate. Relative mRNA abundance for each sample were normalized to those of cyclophilin.

RT-PCR

Total RNA was isolated with RNA STAT60 from cultured cells or rat brain, treated with DNase I, and reverse transcribed using Superscript II RNase H- reverse transcriptase. Each PCR reaction was performed in a reaction volume of 10 uL that contained 5uL GoTaq green (Sigma-Aldrich), 180nM of each PCR primer, and cDNA was added at 20, 4.0, or 0.8 pg per reaction. The reaction conditions were as follows: initial denaturation at 95 °C for 5 min and 3 cycles of amplification (95 °C for 30 s, 60 °C for 30 s and 72 °C for 60 s), followed by 35 cycles of amplification (94 °C for 30 s, 57 °C for 60s and 72 °C for 60 s), followed by a final extension step for 10 min at 72 °C. The PCR reaction products were separated by electrophoresis in a 2.0% agarose gel and stained with ethidium bromide. Relative mRNA abundance for each sample was determined by normalizing the optical density of NTN to that of alpha actin. Total optical densities were quantified using ChemiImager software (Alpha Innotech, San Leandro, CA).

Real-time Quantitative PCR. and RT-PCR Primers

Rat primers sequences are as follows:

Cyclophilin forward:	5′-CCC TGA AGG ATG TGA TCA TTG-3′
Cyclophilin reverse:	5′-GGA AAA GGG TTT CTC CAC TT-3′
Nestin forward:	5′-CAA GTG CCC CCG GTA CTG-3′
Nestin reverse:	5′-TCA GCA AAC CCA TCA GAT TCC-3′
GFAP forward:	5′-TGG CCA CCA GTA ACA TGC A-3′
GFAP reverse:	5′-CAA ACT TGG ACC GAT ACC ACT CT-3′
NeuroD forward:	5′-CCC AGA GGC AGC CAA GTC-3′
NeuroD reverse:	5′-AGC CTT TAG TAA AAC AAT TGA ATG TCT AG-3′
S100beta forward:	5′-ATC AAC AAC GAG CTC TCT CAC TTC-3′
S100beta reverse:	5′-CAC TTC CTG CTC TTT GAT TTC CT-3′
Tuj-1/β-tubulin III forward:	5′-GAG GCC TCC TCT CAC AAG TAT GT-3′
Tuj-1/β-tubulin III reverse:	5′-ACG CTG TCC ATG GTT CCA-3′
VE cadherin forward:	5′-CAC GAC AAT ACC GCC AAC A-3′
VE cadherin reverse:	5′-AAC TTG GTA TGC TCC CGA TTA AA-3′
Persephin forward:	5′-GAC CTG GAA GCC CCA TCA- 3′
Persephin reverse:	5′-GCC GGC ACA AAC CAG GTA- 3′
Artemin forward:	5′-TTG GAG AC CTA CTG CAT TGT C- 3′
Artemin reverse:	5′-CAG CTA GGG TTG GCC ACA AG- 3′
Neurturin forward:	5′-CAG CGG AGG CGC GTG CGC AGA GA -3′
Neurturin reverse:	5′-CGG CTG TGC ACG TCC AGG AAG GA-3′
α-actin forward:	5′-TGT AAG GCG GGC TTT GCT-3′
α-actin reverse:	5′-CCC ACG ATG GAT GGG AAA -3′
Tyrosine hydroxylase forward:	5′-TGT TGG CTG ACC GCA CAT T- 3′
Tyrosine hydroxylase reverse:	5′-GCC CCC AGA GAT GCA AGT C- 3′
Nerve growth factor forward:	5′-CTC TGA GGT GCA TAG CGT AAT GTC-3′
Nerve growth factor reverse:	5′-AAA ACG CTG TGA GAG TGT AGA AC- 3′
Neuron Specific Enolase forward:	5′-GCT TTG CCC CCA ATA TCC T-3′
Neuron Specific Enolase reverse	5′-CCT TGT CAA TGG CTT CCT TCA-3′
Choline acetyltransferase forward:	5′-AGC CAA TCG CTG GTA TGA CA-3′
Choline acetyltransferase reverse:	5′-CAC CGC AGG TGC CAT CT-3′
Smooth muscle alpha actin forward:	5′-TGT AAG GCG GGC TTT GCT- 3′
Smooth muscle alpha actin reverse:	5′-CCC ACG ATG GAT GGG AAA-3′
Ciliary neurotrophic factor forward:	5′-CTG GCT AGC AAG GAA GAT TCG-3′

Ciliary neurotrophic factor reverse:	5′-CAG GCC CTG ATG TTT TAC ATA AGA -3′
Glial-derived neurotrophic factor forward:	5′-CTC CAA TAT GCC CGA AGA TTA TC- 3′
Glial-derived neurotrophic factor reverse:	5′-AGT CTT TTG ATG GTG GCT TGA A -3′
Brain-derived neurotrophic factor forward:	5′-CGC ACC TCT TTA GGC ATC CT -3′
Brain-derived neurotrophic factor reverse:	5′-TCC CGG ATG AAA GTC ACT -3′
Platelet derived growth factor forward:	5′-AAT GAC CAC GGC GAT GAG A- 3′
Platelet derived growth factor reverse:	5′-TCT TCC AGT GTT TCC AGC AGC- 3′
Vascular endothelial growth factor forward:	5′-AAC GAA AGC CGA AGA AAT CC- 3′
Vascular endothelial growth factor reverse:	5′-CGC TCT GAA CAA GGC TCA CA- 3′

Multi-Electrode Arrays (MEAs)

ADAS cells were passaged to P2 plated into D10 on poly-D-lysine coated multielectrode arrays to record any spontaneous or evoked neural network activity as described previously (Keefer, Norton et al. 2001; Mistry, Keefer et al. 2002). Cells were proliferated in D10 supplemented with 10ng/mL EGF and 20ng/mL FGF-2 for 2 days then differentiated by mitogen withdrawal and exposure to the indicated differentiation conditions (NDM or N2/VPA) for 5 days. Application of the excitatory neurotransmitter glutamate (5 μM), the GABA A receptor antagonist bicuculline (20 μM), or trains of electrical stimulation (0.75 V biphasic pulses, trains of 10 pulses repeated 5 times with 30 seconds between pulse trains) were performed to evoke neural network activity.

Statistical Analyses

Intergroup differences among the means between the various dependent variables were analyzed using one-way ANOVA. When ANOVA showed significant differences, comparisons between means were tested by Tukey's multiple-comparison post hoc test (Graph Pad Prism, San Diego, CA). Values expressed are the group means ± S.E.M or group means ± S.D. as indicated. Groups represented by histogram bars labeled with different letters are significantly different at $p < 0.05$. Groups with asterisks (*) are significantly different from sham-transplanted group at $p < 0.05$.

Results

Morphological differentiation and expression of neuro-glial markers in naïve and differentiated ADAS cells *in vitro*

The initial selection of the adipose stromal cell population at P0 was accomplished by retaining a relatively small fraction of adherent cells (<10%) and discarding non-adherent cells 24 hrs after plating. In agreement with previous reports, we were able to grow and expand flat and fibroblast-like adipose-derived adult stromal (ADAS) *in vitro* with high efficiency for a number of passages (~P15). Pre-exposure to a mitogenic cocktail consisting of EGF/FGF-2 promoted expansion of a spindle-shaped putative progenitor pool within the heterogenous stromal cell population. To induce differentiation, the mitogenic cocktail was withdrawn and cells were exposed to serum-containing Neural Differentiation Medium (NDM) or to the histone deacetylase inhibitor valproic acid (VPA) in N2-supplemented serum free medium. The latter was chosen because exposure to VPA/N2 *in vitro* has been shown to induce neuronal differentiation of adult hippocampal neural progenitors via expression of the neurogenic basic helix-loop-helix transcription factor NeuroD (Hsieh, Nakashima et al. 2004). Under these treatment conditions, a large fraction (>50% of total cells) of the cells in ADAS cultures pre-induced with EGF/FGF-2 for 24 hrs displayed bipolar and multipolar morphologies with extensive process outgrowth (Figures 1 and 5) appearing by 12 hrs compared to cells not pre-induced with the mitogenic cocktail (5% of total cells) in agreement with morphological differentiation described by others (Ashjian, Elbarbary et al. 2003; Safford, Safford et al. 2004).

Prior to embarking on transplantation studies, we first established the extent to which the morphological differentiation of ADAS cells into neuron-like cells was coincident with expression of cellular markers of differentiation. Two-day treatment with EGF/FGF-2 induced expression of markers characteristic of early neural progenitors (including nestin, vimentin, and glial fibrillary acidic protein) in a significant fraction of the cells (Table 1). Molecular markers denoting early commitment to neuronal fates such as β-tubulin III/Tuj1 and neuron specific enolase (NSE) were detectable in a significant fraction of cells only after exposure to NDM or N2/VPA (Figure 1, Table 1, Supplemental Figure 1). Molecular markers of mature neurons, including neuronal N antigen (NeuN), microtubule-associated protein-2 (MAP2), TrkB, tyrosine hydroxylase (TH), choline acetyltransferase (ChAT), and gamma amino butyric acid (GABA) were detected with low frequency in a small population of the cells treated with either differentiation medium and supplemented with factors such as brain-derived neurotrophic factor (BDNF) or glial-derived neurotrophic factor (GDNF) and did not increase further with additional time (7–10 days) in culture (Supplemental Figure 1). Lastly, expression of Smooth Muscle Actin (SMA) and the endothelial cell marker VE cadherin was detectable in a subpopulation of the cells after proliferation in EGF/FGF-2 and after NDM treatment (Table 1, Supplemental Figure 1). As indicated in Table 1, mRNA expression of several of these protein markers was confirmed by real-time quantitative PCR analysis (data not shown). These findings are in agreement with reports made for adipose-derived stromal cells from humans, rodents, and non-human primates (Safford, Hicok et al. 2002;Zuk, Zhu et al. 2002;Ashjian, Elbarbary et al. 2003;Safford, Safford et al. 2004;Fujimura, Ogawa et al. 2005;Romanov, Darevskaya et al. 2005;Ning, Lin et al. 2006).

Autologous ADAS cell grafts attenuate 6-OHDA-induced nigrostriatal pathway degeneration and behavioral deficits

Given that ADAS cells can be coaxed to display morphological, molecular, and cellular markers characteristic of neuroblasts in response to two different neuritizing cocktails, the critical question is whether neural induction of ADAS *in vitro* prior to transplantation is required to derive therapeutic benefit from autologous ADAS grafts in a rat model of Parkinson's disease. To ensure that ADAS cells could be tracked after autologous transplantation to assess ADAS engraftment and neuronal differentiation in brain sections upon completion of the study, we conducted pilot experiments to select a stable cell labeling method that did not compromise cell viability. ADAS cells were harvested from adult rats, expanded *in vitro* to passage 2 with EGF/FGF-2, and pre-labeled with the fixable mitochondrial-specific probe CMX-H2 MitoTracker Red (MTR) before prior to transplantation. We found that ADAS transplants were able to survive, engraft, and retain MTR fluorescence in unlesioned animals for at least three weeks (Supplemental Figure 2). Importantly, because MTR fluorescence in cells requires an intact mitochondrial membrane potential, this cell labeling method enabled us to track and identify *in situ* only those cells which were viable and healthy. Labeling of ADAS cells with a lentivirus encoding Green Fluorescent Protein (GFP) confirmed these findings but was not chosen for these studies to avoid the potential toxicity of GFP overexpression. In addition, GFP fluorescence does not depend on the viability of the cells and could have confounded interpretation of survival and engraftment studies.

Next, we investigated the ability of autologous ADAS cell transplants to protect, repair or restore function in a model of Parkinson's disease (PD). We chose a model in which there is progressive degeneration of the nigrostriatal pathway for at least three weeks following a neurotoxic injury induced by striatal injection of 6-hydroxydopamine (6-OHDA) (Kirik, Rosenblad et al. 1998). Autologous transplants of naïve or differentiated (NDM-treated) ADAS cells were injected into the rostral midbrain one week after striatal 6-OHDA admistration while the lesion was still progressing. The extent of the nigrostriatal lesion was evaluated prior to transplantation and weekly thereafter using a standard amphethamine-induced rotational

behavior test. Quantitative stereological analyses of TH-positive neuron number in SNpc indicated that the group of 6-OHDA-lesioned rats that received nigral ADAS grafts displayed significantly reduced loss of TH-immunoreactive neurons on the lesioned side 4 weeks post-transplantation compared to sham-transplanted 6-OHDA lesioned rats (Figure 2a and b, Supplemental Table 1). In addition, quantification of TH-positive fiber density in the striatum indicated that ADAS cell transplants spared striatal terminals; specifically, 6-OHDA-lesioned/sham transplanted animals displayed 35% of control versus 65–72% of control in 6-OHDA-lesioned/ADAS-transplanted animals (Figure 2c). It is difficult to ascertain with certainty whether the increased TH-immunoreactivity in the ADAS cell-transplanted animals reflects true sparing of terminals, re-growth, and/or attenuated down-regulation of TH expression induced by 6-OHDA neurotoxicity, but we speculate it may be a combination of all three processes. Importantly, neurohistological protection by ADAS cell transplants was accompanied by improvement in locomotor deficits. Behavioral analyses indicated that 6-OHDA-lesioned rats that received naïve or differentiated ADAS cell transplants displayed significantly attenuated amphetamine-induced rotational behavior compared to sham-transplanted rats that received no ADAS cells (Figure 2d), suggesting that ADAS grafts prevented the progressive retrograde degeneration of the nigrostriatal pathway and contributed to striatal dopamine preservation. To our knowledge, this is the first demonstration that autologous transplantation of ADAS cells provides robust protection to rostral midbrain dopaminergic neurons against oxidative neurotoxins independent of the pre-differentiation status of the cells. Similar neuroprotective effects of ADAS cells have been reported in stroke and spinal cord injury models using rat, non-human primate, and human adipose-derived adult stromal cell populations (Kang, Lee et al. 2003; Tansey 2005; Kang, Shin et al. 2006).

ADAS cells survive after transplantation but do not differentiate into dopaminergic neurons

The equivalent degree of nigral dopaminergic neuron protection achieved by transplantation of either naïve or NDM differentiated ADAS into hemi-parkinsonian rats suggested that the pre-transplantation differentiation status of the cells did not determine their ability to survive or neuroprotect *in vivo* after transplantation. This observation led us to hypothesize that either both types of grafts had undergone robust differentiation into dopaminergic fates *in vivo* and partially replaced the lost nigral dopaminergic neurons; or alternatively, that the neurally induced ADAS cells failed to maintain the neural phenotypes *in vivo* but afforded neuroprotection to the same extent as the naïve ADAS cells, implying that a mechanism other than cell replacement had contributed to functional recovery in the hemi-parkinsonian rats. To distinguish between these two mutually exclusive possibilities, we performed immunohistological analyses of midbrain sections. Four weeks after transplantation, examination of brain cryosections revealed the presence of MTR-labeled ADAS cells in close proximity to TH-positive neurons in substantia nigra; however, co-expression of TH (or any other neural markers) and MTR was not detected (Figure 3a–c). On the basis of these findings we concluded that neuroprotection by ADAS cells was achieved without them adopting dopaminergic neuron fates *in vivo.*

ADAS cell transplants attenuate microglial activation in SNpc of 6-OHDA-lesioned animals

Because neuroinflammation has been implicated in the progressive degeneration of the nigrostriatal pathway in humans and in experimental models of PD (reviewed in (Hunot and Hirsch 2003; Hald and Lotharius 2005; Whitton 2007) and previous work from our laboratory implicated microglial-derived soluble TNF as a critical mediator of nigral dopaminergic neuron loss induced by 6-OHDA (McCoy, Martinez et al. 2006), we aimed to determine whether ADAS cell transplants had a modulatory effect on the neuroinflammatory reaction in the nigrostriatal pathway following a 6-OHDA lesion. Immunohistological analyses of the microglial activation markers OX-42 and F4/80 in SNpc of unlesioned, 6-OHDA-lesioned/sham-transplanted, and 6-OHDA-lesioned ADAS cell-transplanted animals indicated

attenuation of the neuroinflammatory response 4 weeks post-transplant in animals that received the ADAS cell transplants compared to lesioned animals that received a sham-transplant (Figure 3d). Specifically, quantification of microglial burden in SNpc indicated a reduction in microglial burden of 45% (Figure 3e). Although not direct proof that ADAS cells produced anti-inflammatory mediators in the nigral environment, these data raise the interesting possibility that ADAS cell-derived molecular mediators may have the capacity to influence microglial activity at a site of injury.

Phenotypic stability, cell cycle exit, and terminal differentiation of ADAS cells *in vitro*

The lack of detectable differentiation of ADAS into DA neurons after transplantation left us to consider the alternative hypothesis that ADAS cell differentiation induced *in vitro* was short-lived *in vivo* and both naïve and NDM-treated cell types afforded neuroprotection through a mechanism unrelated to their ability to adopt neuronal fates. We sought empirical support for this hypothesis by investigating the relative stability of the *in vitro* differentiated ADAS phenotypes after re-exposure to serum-containing medium. We monitored P2 and P3 cultures for changes in expression of the early neural progenitor marker nestin and the nuclear proliferation marker Ki67 in ADAS cell cultures grown in serum-containing medium D10, in response to mitogens (EGF and FGF-2), after 4- or 7-day neural induction in NDM, and following re-exposure to D10 for 1 or 2 days. Expression of the nuclear proliferation antigen Ki67 (Figure 4a and b) and nestin (Figure 4c) increased upon stimulation with mitogens, decreased after 4 days in differentiation media, and continued to decline by 7 days in the same; while expression of the neuronal commitment marker Tuj-1 (Figure 4d) was increased in a small fraction of the cells in response to mitogens, peaked in differentiation media after 4 days (see also Table 1) and remained highly expressed at 7 days. However, re-exposure of differentiated cultures to serum-containing medium induced a second wave of proliferation evidenced by Ki67 (Figure 4a and b) and nestin (Figure 4c) re-emergence in the cultures; concomitantly, Tuj-1 expression (Figure 4d) began to decline immediately to levels below those observed after 7 days in NDM. Taken together, these findings indicate that the *in vitro* differentiated ADAS cell phenotypes induced by the neuritizing cocktails NDM are relatively unstable. Mechanistically, this plasticity is consistent with the possibility that NDM-treated ADAS cells lost their neurally-induced phenotypes *in situ* after transplantation. To extend and confirm the observations that neurally induced ADAS cells do not display characteristics of terminally differentiated neurons, we exposed ADAS cell cultures to a 4-day treatment of VPA-supplemented N2 serum-free medium, conditions previously reported to induce terminal differentiation of neural stem cells (Hsieh, Nakashima et al. 2004). Consistent with results obtained after exposure to NDM, ADAS did not become terminally differentiated into mature neurons after exposure to N2/VPA as evidenced by persistent expression of the transcription factor NeuroD (Figure 5, top panel) which is present in neuroblasts during the early stages of neural lineage commitment (Katayama, Mizuta et al. 1997; Amrein, Slomianka et al. 2004). Moreover, exposure to NDM induced outgrowth of processes in a subpopulation of the cells in the culture; yet these cells continued to express Ki67 (Figure 5, white ovals) much like cells treated with the mitogenic cocktail EGF/FGF-2 in D10. In fact, proliferation arrest in NDM-treated cultures was not evident in morphologically differentiated cells until supplementation with agents that induce rapid and robust differentiation of neuroblasts into mature neurons (i.e., all-trans retinoic acid and forskolin); under these conditions, only flat fibroblast-like undifferentiated cells without processes continued to cycle (Figure 5, white rectangles). Together with results from experiments addressing phenotypic stability, these findings suggest that neural induction of ADAS cells *in vitro* prior to transplantation does not induce terminal differentiation of ADAS into mature neurons. Given that morphological and molecular differentiation status of ADAS cells is determined by the strength and duration of the differentiation signal, supraphysiological stimuli may be required for ADAS to undergo terminal differentiation and cell cycle exit.

ADAS cell cultures do not display spontaneous or evoked electrical activity *in vitro*

Next, we investigated the extent to which morphological differentiation of ADAS cells correlated with functional differentiation of ADAS cells into mature neurons. Upon elevation of extracellular potassium to 20mM, a subset of morphologically differentiated ADAS cells responded to depolarizing stimuli by increasing intracellular free calcium concentrations as measured by increasing fluorescence intensity of the calcium indicator fluo-4 (data not shown), consistent with published reports that ADAS obtained from human processed lipo-aspirates express a delayed-rectifier type K+ current expressed during early neuronal development (Ashjian, Elbarbary et al. 2003). However, attempts to measure spontaneous or evoked action potentials via intracellular recordings were unsuccessful. Likewise, attempts to measure spontaneous neural network activity from ADAS cells grown on multi-electrode arrays (MEAs) or evoked activity in response to glutamate (5 μM), the GABA A receptor antagonist bicuculline (20 μM), or trains of electrical stimulation (0.75 V biphasic pulses, trains of 10 pulses repeated 5 times with 30 seconds between pulse trains) in NDM or N2/VPA-treated cells were also unsuccessful (data not shown) despite their differentiated morphology (i.e., extended processes) (Supplemental Figure 3). Taken together, our findings indicate that terminal differentiation of ADAS cells into electrically mature neurons does not occur *in vitro* under the conditions tested. In this respect, our results are similar to those reported for multipotent skin-derived progenitor (SKP) cells which express neuro-glial markers but fail to progress from neuroblast to neuron-like stages *in vitro* (Fernandes, Kobayashi et al. 2006), possibly due to lack of electrical stimulation (Waragai, Wei et al. 2006) or other critical signaling cues which may be possible *in vivo* through interactions with endogenous cell populations.

ADAS cells express neurotrophic factors that protect dopaminergic neurons and promote their survival

We hypothesized that one mechanism by which transplanted ADAS grafts could contribute to attenuated DA neuron loss after toxin-induced death without undergoing terminal differentiation into DA neurons might be through production of trophic factors at the site of injury that can protect DA neurons and promote their survival and/or differentiation of endogenous progenitor populations into dopaminergic neurons. On the basis of previous work (Milbrandt, de Sauvage et al. 1998), we determined that the most likely candidates to examine would be the glial-derived neurotrophic factor (GDNF) family ligands (GFLs), brain-derived neurotrophic factor (BDNF), and nerve growth factor (NGF) because multiple *in vitro* and *in vivo* studies have demonstrated their ability to protect dopaminergic neurons and/or help repair a damaged nigrostriatal pathway. To test this idea, we performed real-time quantitative PCR analysis (or RT-PCR in the case on NTN) of ADAS cells proliferated *in vitro* in the presence of EGF/FGF-2 for the exact amount of time as cells used in transplantation studies. We found that ADAS cells express high levels of mRNA for BDNF, GNDF, and NGF relative to the levels normally detected in rat brain (Figure 6). All of these factors exert potent trophic and neuroprotective effects on nigral dopaminergic neurons (Stromberg, Herrera-Marschitz et al. 1985; Hyman, Hofer et al. 1991; Lin, Doherty et al. 1993). Levels of these neuroprotective growth factors were generally highest in EGF/FGF-2 expanded cultures. These *in vitro* findings suggest one possible mechanism by which autologous ADAS cell transplants might have mediated neuroprotection.

Discussion

Several studies to date have reported that Adipose-Derived Adult Stromal (ADAS) cells from rats (Tholpady, Katz et al. 2003; Yang, Liu et al. 2004; Ning, Lin et al. 2006), mice (Safford, Hicok et al. 2002; Fujimura, Ogawa et al. 2005), rhesus monkeys (Kang, Putnam et al. 2004), and humans (Safford, Hicok et al. 2002; Zuk, Zhu et al. 2002; Ashjian, Elbarbary et al. 2003;

Kang, Jun et al. 2003; Fujimura, Ogawa et al. 2005) can be coaxed to differentiate into neuron-like morphologies and to express neuro-glial markers *in vitro*. Importantly, our study is the first to demonstrate that *in vitro* neural induction and stable terminal differentiation of ADAS cells into functionally mature neurons *in vivo* are not necessary for ADAS cells to exert neuroprotective effects in models of neurological injury and thus be considered viable tissue sources to treat neurodegenerative diseases. It was somewhat surprising that the neuroprotective effects achieved in our studies were derived from transplantation of a small number of naïve or neurally-induced ADAS cells (~40,000). However, neuroprotective effects in hemi-parkinsonian rats have also been reported with small numbers of bone marrow-derived stromal (BMSC) (Dezawa, Kanno et al. 2004; Aggarwal, Shishodia et al. 2006; Hellmann, Panet et al. 2006). We have not transplanted 6-OHDA-lesioned animals with ADAS cells at any other time-point during the lesion; but we predict that if ADAS cells can survive in the hostile oxidative and neuroinflammatory environment of the SNpc during the first week after a striatal 6-OHDA injection, they are likely to survive at a later date. Future experiments will investigate whether delayed transplantation of ADAS cells affords similar neuroprotective effects.

Ideally, viable sources for cell replacement therapies in neurological disease would limit the magnitude of injury or degeneration or their sequelae, replace lost neurotransmitters, secrete neurotrophic factors or neuromodulatory substances to promote proliferation and survival of endogenous precursors, or promote restoration of function in neural circuits. Successful outcomes of neural stem cell grafts in restoration of function after 6-OHDA-induced nigrostriatal degeneration has been attributed to a combination of neural differentiation and trophic factor production (Yasuhara, Matsukawa et al. 2006) in large part based on the observation that a large fraction of adult neural stem cells within transplanted grafts retain detectable nestin expression and never fully mature post-transplantation. Likewise, the *in vivo* neuroprotective effects of other cell types with demonstrated *in vitro* multi-lineage potential, including mesenchymal stem cells (MSC) (Scuteri, Cassetti et al. 2006), umbilical cord matrix stem cells (Weiss, Medicetty et al. 2006), and bone marrow derived stromal cells (BMSCs) (Garcia, Aguiar et al. 2004; Carvey, Chen et al. 2005; Ye, Chen et al. 2005), has been shown to be mediated in part through a mechanism of trophic support.

ADAS cells may have afforded neurohistological protection and ameliorated functional deficits induced by the striatal 6-OHDA lesion through multiple mechanisms. Our findings from *in vitro* studies on neurotrophic factor gene expression suggest that one likely mechanism by which both kinds of ADAS cell grafts may have contributed to neuroprotection or attenuated dopaminergic dysfunction and neuronal loss in the 6-OHDA rat model is through production of neurotrophic factors at the lesion site. Consistent with this idea, NGF has been shown to promote survival of fetal ventral mesencephalic cells and rescue dopaminergic neurons (Chaturvedi, Shukla et al. 2006; Kavanagh, Loughlin et al. 2006) and its mRNA expression in neurally-induced and naïve ADAS cells was approximately 2- and 30-fold, respectively that of total brain. Secretion of BDNF by engineered fibroblasts transplanted into the striatum has been shown to attenuate loss of dopaminergic neuron cell bodies within the SN pars compacta induced by striatal 6-OHDA injection (Levivier, Przedborski et al. 1995). Notably, ADAS cells expressed this and other potent dopaminergic survival factor *in vitro*. Specifically, BDNF and GDNF expression in ADAS cells was 2- to 4-fold that of total brain; we posit that secretion of these potent trophic factors *in situ* may have contributed to protection of vulnerable DA neurons. Similarly, BMSCs engineered with Neurturin were reported to reduce striatal dopamine deficiency and rotational behavior without significantly affecting 6-OHDA-induced TH-neuron loss (Ye, Wang et al. 2007). In the future, it may in fact be possible to augment the neuroprotective effects of ADAS grafts in the nigrostriatal pathway even further by enginnering them to secrete more of these factors. In support of this idea, human ADAS grafts transduced with an adenovirus encoding BDNF improved functional deficits in a model of stroke (Kang,

Lee et al. 2003). Other mechanisms that have been proposed to explain the neurorestorative properties of ADAS cells in other studies include stimulation of migration and proliferation of endogenous neural precursor populations to the lesion site and production of pro-angiogenic factors including VEGF, hepatocyte growth factor, or TGFβ (Rehman, Traktuev et al. 2004).

In summary, non-engineered ADAS cells may never replace neural stem cells or embryonic cells as a source of multipotent neural progeny for cell replacement therapies to treat CNS diseases. Nevertheless, the discovery that a stromal cell population residing in adult adipose, a tissue of mesodermal origin that is readily accessible and easy to harvest, displays molecular properties of neural progenitor cells *in vitro* and neuroprotective properties *in vivo* has important basic science and clinical implications. Critical advances in the field of neurorestorative medicine may soon be possible due to the identification of adult adipose as a novel non-immunogenic and easy-to-harvest tissue source that contains large numbers of cells with neuroprotective properties towards dopaminergic neurons that can be expanded *in vitro* for autologous transplantation. In addition to the inherent non-immunogenic properties of autologous ADAS grafts and their demonstrated neuroprotective capacity, we predict that the latter could be enhanced further by genetic engineering with GFLs. Alternatively, engineering of ADAS cells with neuroimmune modulatory peptides may also warrant investigation in pre-clinical models of PD in light of the overwhelming amount of recent evidence implicating neuroinflammatory processes in the progressive degeneration of the nigrostriatal pathway and development of PD in humans (reviewed in (Tansey, McCoy et al. 2007; Whitton 2007).

Supplementary Material

Refer to Web version on PubMed Central for supplementary material.

Acknowledgements

This work was supported by grants from the National Parkinson Foundation (MGT), the National Institute of Neurological Disorders and Stroke, National Institutes of Health (R21 NS051526-02, MGT and KET), and a National Institutes of Health Predoctoral Training Grant GM007062 (PCW). We would like to thank John Hong for technical help with immunocytochemistry, Christine Smith for help with surgery and animal care, and members of the Tansey labs for helpful discussions. We would also like to thank Dr. Don Cooper in the Department of Psychiatry at UT Southwestern for access to his StereoInvestigator system.

References

Aggarwal BB, Shishodia S, et al. TNF blockade: an inflammatory issue. Ernst Schering Res Found Workshop 2006;(56):161–86. [PubMed: 16331857]

Alison M, Sarraf C. Hepatic stem cells. J Hepatol 1998;29(4):676–82. [PubMed: 9824279]

Amoh Y, Li L, et al. Multipotent nestin-positive, keratin-negative hair-follicle bulge stem cells can form neurons. Proc Natl Acad Sci U S A 2005;102(15):5530–4. [PubMed: 15802470]

Amrein I, Slomianka L, et al. Marked species and age-dependent differences in cell proliferation and neurogenesis in the hippocampus of wild-living rodents. Hippocampus 2004;14(8):1000–10. [PubMed: 15390172]

Ashjian PH, Elbarbary AS, et al. In vitro differentiation of human processed lipoaspirate cells into early neural progenitors. Plast Reconstr Surg 2003;111(6):1922–31. [PubMed: 12711954]

Belmadani A, Tran PB, et al. Chemokines regulate the migration of neural progenitors to sites of neuroinflammation. J Neurosci 2006;26(12):3182–91. [PubMed: 16554469]

Bonilla S, Silva A, et al. Functional neural stem cells derived from adult bone marrow. Neuroscience 2005;133(1):85–95. [PubMed: 15893633]

Bossolasco P, Cova L, et al. Neuro-glial differentiation of human bone marrow stem cells in vitro. Exp Neurol 2005;193(2):312–25. [PubMed: 15869934]

Burke RE, Cadet JL, et al. An assessment of the validity of densitometric measures of striatal tyrosine hydroxylase-positive fibers: relationship to apomorphine-induced rotations in 6-hydroxydopamine lesioned rats. J Neurosci Methods 1990;35(1):63–73. [PubMed: 1980518]

Carvey PM, Chen EY, et al. Intra-parenchymal injection of tumor necrosis factor-alpha and interleukin 1-beta produces dopamine neuron loss in the rat. J Neural Transm 2005;112(5):601–12. [PubMed: 15583962]

Chaturvedi RK, Shukla S, et al. Nerve growth factor increases survival of dopaminergic graft, rescue nigral dopaminergic neurons and restores functional deficits in rat model of Parkinson's disease. Neurosci Lett 2006;398(1–2):44–9. [PubMed: 16423459]

Conti L, Reitano E, et al. Neural stem cell systems: diversities and properties after transplantation in animal models of diseases. Brain Pathol 2006;16(2):143–54. [PubMed: 16768755]

Dezawa M, Kanno H, et al. Specific induction of neuronal cells from bone marrow stromal cells and application for autologous transplantation. J Clin Invest 2004;113(12):1701–1710. [PubMed: 15199405]

Easterday MC, Dougherty JD, et al. Neural progenitor genes. Germinal zone expression and analysis of genetic overlap in stem cell populations. Dev Biol 2003;264(2):309–22. [PubMed: 14651920]

Fernandes KJ, Kobayashi NR, et al. Analysis of the neurogenic potential of multipotent skin-derived precursors. Exp Neurol 2006;201(1):32–48. [PubMed: 16678161]

Fernandes KJ I, McKenzie A, et al. A dermal niche for multipotent adult skin-derived precursor cells. Nat Cell Biol 2004;6(11):1082–93. [PubMed: 15517002]

Frankel MS. In search of stem cell policy. Science 2000;287(5457):1397. [PubMed: 10722382]

Fujimura J, Ogawa R, et al. Neural differentiation of adipose-derived stem cells isolated from GFP transgenic mice. Biochem Biophys Res Commun 2005;333(1):116–21. [PubMed: 15939405]

Gage FH. Mammalian neural stem cells. Science 2000;287(5457):1433–8. [PubMed: 10688783]

Gage FH, Ray J, et al. Isolation, characterization, and use of stem cells from the CNS. Annu Rev Neurosci 1995;18:159–92. [PubMed: 7605059]

Garcia R, Aguiar J, et al. Bone marrow stromal cells produce nerve growth factor and glial cell line-derived neurotrophic factors. Biochem Biophys Res Commun 2004;316(3):753–4. [PubMed: 15033464]

German DC, Manaye KF. Midbrain dopaminergic neurons (nuclei A8, A9, and A10): three-dimensional reconstruction in the rat. J Comp Neurol 1993;331(3):297–309. [PubMed: 8514911]

Guilak F, Lott KE, et al. Clonal analysis of the differentiation potential of human adipose-derived adult stem cells. J Cell Physiol 2006;206(1):229–37. [PubMed: 16021633]

Hald A, Lotharius J. Oxidative stress and inflammation in Parkinson's disease: is there a causal link? Exp Neurol 2005;193(2):279–90. [PubMed: 15869932]

Hellmann MA, Panet H, et al. Increased survival and migration of engrafted mesenchymal bone marrow stem cells in 6-hydroxydopamine-lesioned rodents. Neurosci Lett 2006;395(2):124–8. [PubMed: 16359791]

Hermann A, Gastl R, et al. Efficient generation of neural stem cell-like cells from adult human bone marrow stromal cells. J Cell Sci 2004;117(Pt 19):4411–22. [PubMed: 15304527]

Hermann A, Gerlach M, et al. Neurorestoration in Parkinson's disease by cell replacement and endogenous regeneration. Expert Opin Biol Ther 2004;4(2):131–43. [PubMed: 14998773]

Hermann A, Maisel M, et al. Epigenetic conversion of human adult bone mesodermal stromal cells into neuroectodermal cell types for replacement therapy of neurodegenerative disorders. Expert Opin Biol Ther 2006;6(7):653–70. [PubMed: 16805706]

Hsieh J, Nakashima K, et al. Histone deacetylase inhibition-mediated neuronal differentiation of multipotent adult neural progenitor cells. Proc Natl Acad Sci U S A 2004;101(47):16659–64. [PubMed: 15537713]

Hunot S, Hirsch EC. Neuroinflammatory processes in Parkinson's disease. Ann Neurol 2003;53(Suppl 3):S49–58. [PubMed: 12666098]discussion S58–60

Hyman C, Hofer M, et al. BDNF is a neurotrophic factor for dopaminergic neurons of the substantia nigra. Nature 1991;350(6315):230–2. [PubMed: 2005978]

Izadpanah R, Trygg C, et al. Biologic properties of mesenchymal stem cells derived from bone marrow and adipose tissue. J Cell Biochem 2006;99(5):1285–97. [PubMed: 16795045]

Jiang Y, Jahagirdar BN, et al. Pluripotency of mesenchymal stem cells derived from adult marrow. Nature 2002;418(6893):41–9. [PubMed: 12077603]

Jiang Y, Vaessen B, et al. Multipotent progenitor cells can be isolated from postnatal murine bone marrow, muscle, and brain. Exp Hematol 2002;30(8):896–904. [PubMed: 12160841]

Kang SK, Jun ES, et al. Interactions between human adipose stromal cells and mouse neural stem cells in vitro. Brain Res Dev Brain Res 2003;145(1):141–9.

Kang SK, Lee DH, et al. Improvement of neurological deficits by intracerebral transplantation of human adipose tissue-derived stromal cells after cerebral ischemia in rats. Exp Neurol 2003;183(2):355–66. [PubMed: 14552877]

Kang SK, Putnam LA, et al. Neurogenesis of Rhesus adipose stromal cells. J Cell Sci 2004;117(Pt 18): 4289–99. [PubMed: 15292397]

Kang SK, Shin MJ, et al. Autologous adipose tissue-derived stromal cells for treatment of spinal cord injury. Stem Cells Dev 2006;15(4):583–94. [PubMed: 16978061]

Katayama M, Mizuta I, et al. Differential expression of neuroD in primary cultures of cerebral cortical neurons. Exp Cell Res 1997;236(2):412–7. [PubMed: 9367625]

Kavanagh ET, Loughlin JP, et al. Functionality of NGF-protected PC12 cells following exposure to 6-hydroxydopamine. Biochem Biophys Res Commun 2006;351(4):890–5. [PubMed: 17092485]

Keefer EW, Norton SJ, et al. Acute toxicity screening of novel AChE inhibitors using neuronal networks on microelectrode arrays. Neurotoxicology 2001;22(1):3–12. [PubMed: 11307849]

Kirik D, Rosenblad C, et al. Characterization of behavioral and neurodegenerative changes following partial lesions of the nigrostriatal dopamine system induced by intrastriatal 6-hydroxydopamine in the rat. Exp Neurol 1998;152(2):259–77. [PubMed: 9710526]

Kurrasch DM, Huang J, et al. Quantitative real-time polymerase chain reaction measurement of regulators of G-protein signaling mRNA levels in mouse tissues. Methods Enzymol 2004;389:3–15. [PubMed: 15313556]

Lakshmipathy U, Verfaillie C. Stem cell plasticity. Blood Rev 2005;19(1):29–38. [PubMed: 15572215]

Levivier M, Przedborski S, et al. Intrastriatal implantation of fibroblasts genetically engineered to produce brain-derived neurotrophic factor prevents degeneration of dopaminergic neurons in a rat model of Parkinson's disease. J Neurosci 1995;15(12):7810–20. [PubMed: 8613721]

Lin LF, Doherty DH, et al. GDNF: a glial cell line-derived neurotrophic factor for midbrain dopaminergic neurons. Science 1993;260(5111):1130–2. [PubMed: 8493557]

McCoy MK, Martinez TN, et al. Blocking soluble Tumor Necrosis Factor signaling with dominant-negative TNF inhibitor attenuates loss of dopaminergic neurons in models of Parkinsons Disease. J Neurosci 2006;26(37):9365–9375. [PubMed: 16971520]

Milbrandt J, de Sauvage FJ, et al. Persephin, a novel neurotrophic factor related to GDNF and neurturin. Neuron 1998;20(2):245–53. [PubMed: 9491986]

Miller RH. The promise of stem cells for neural repair. Brain Res 2006;1091(1):258–64. [PubMed: 16563359]

Mistry SK, Keefer EW, et al. Cultured rat hippocampal neural progenitors generate spontaneously active neural networks. Proc Natl Acad Sci U S A 2002;99(3):1621–6. [PubMed: 11818538]

Ning H, Lin G, et al. Neuron-like differentiation of adipose tissue-derived stromal cells and vascular smooth muscle cells. Differentiation 2006;74(9–10):510–8. [PubMed: 17177848]

Paxinos G, Watson C, et al. Bregma, lambda and the interaural midpoint in stereotaxic surgery with rats of different sex, strain and weight. J Neurosci Methods 1985;13(2):139–43. [PubMed: 3889509]

Paxinos, GaWC. The rat brain in stereotaxic coordinates. Academic Press; 1998.

Poot M, Zhang YZ, et al. Analysis of mitochondrial morphology and function with novel fixable fluorescent stains. J Histochem Cytochem 1996;44(12):1363–72. [PubMed: 8985128]

Potten CS. Stem cells in gastrointestinal epithelium: numbers, characteristics and death. Philos Trans R Soc Lond B Biol Sci 1998;353(1370):821–30. [PubMed: 9684279]

Rehman J, Traktuev D, et al. Secretion of Angiogenic and Antiapoptotic Factors by Human Adipose Stromal Cells. Circulation 2004;109(10):1292–1298. [PubMed: 14993122]

Romanov YA, Darevskaya AN, et al. Mesenchymal stem cells from human bone marrow and adipose tissue: isolation, characterization, and differentiation potentialities. Bull Exp Biol Med 2005;140(1): 138–43. [PubMed: 16254640]

Safford KM, Hicok KC, et al. Neurogenic differentiation of murine and human adipose-derived stromal cells. Biochem Biophys Res Commun 2002;294(2):371–9. [PubMed: 12051722]

Safford KM, Safford SD, et al. Characterization of neuronal/glial differentiation of murine adipose-derived adult stromal cells. Exp Neurol 2004;187(2):319–28. [PubMed: 15144858]

Schaffler A, Buchler C. Concise review: adipose tissue-derived stromal cells--basic and clinical implications for novel cell-based therapies. Stem Cells 2007;25(4):818–27. [PubMed: 17420225]

Scuteri A, Cassetti A, et al. Adult mesenchymal stem cells rescue dorsal root ganglia neurons from dying. Brain Res 2006;1116(1):75–81. [PubMed: 16959225]

Sonntag KC, Sanchez-Pernaute R. Tailoring human embryonic stem cells for neurodegenerative disease therapy. Curr Opin Investig Drugs 2006;7(7):614–8.

Stromberg I, Herrera-Marschitz M, et al. Chronic implants of chromaffin tissue into the dopamine-denervated striatum. Effects of NGF on graft survival, fiber growth and rotational behavior. Exp Brain Res 1985;60(2):335–49. [PubMed: 4054276]

Tansey KE, McCoy MK, Martinez T, Warren M, Botterman BR, Tansey MG. Adipose Derived Neural Progenitor (ADNP) Cells: A novel source for cell replacement therapy in spinal cord injury. J Neurotrauma 2005;22:1176.

Tansey MG, McCoy MK, et al. Neuroinflammatory mechanisms in Parkinson's disease: Potential environmental triggers, pathways, and targets for early therapeutic intervention. Exp Neurol. 200710.1016/j.expneurol.2007.07.004

Tholpady SS, Katz AJ, et al. Mesenchymal stem cells from rat visceral fat exhibit multipotential differentiation in vitro. Anat Rec A Discov Mol Cell Evol Biol 2003;272(1):398–402. [PubMed: 12704697]

Ungerstedt U, Arbuthnott GW. Quantitative recording of rotational behavior in rats after 6-hydroxy-dopamine lesions of the nigrostriatal dopamine system. Brain Res 1970;24(3):485–93. [PubMed: 5494536]

Waragai M, Wei J, et al. Increased level of DJ-1 in the cerebrospinal fluids of sporadic Parkinson's disease. Biochem Biophys Res Commun 2006;345(3):967–72. [PubMed: 16707095]

Weiss ML, Medicetty S, et al. Human umbilical cord matrix stem cells: preliminary characterization and effect of transplantation in a rodent model of Parkinson's disease. Stem Cells 2006;24(3):781–92. [PubMed: 16223852]

Weissman IL. Translating stem and progenitor cell biology to the clinic: barriers and opportunities. Science 2000;287(5457):1442–6. [PubMed: 10688785]

Weissman IL, Anderson DJ, et al. Stem and progenitor cells: origins, phenotypes, lineage commitments, and transdifferentiations. Annu Rev Cell Dev Biol 2001;17:387–403. [PubMed: 11687494]

West MJ, Slomianka L, et al. Unbiased stereological estimation of the total number of neurons in the subdivisions of the rat hippocampus using the optical fractionator. Anat Rec 1991;231(4):482–97. [PubMed: 1793176]

Whitton PS. Inflammation as a causative factor in the aetiology of Parkinson's disease. Br J Pharmacol 2007;150(8):963–76. [PubMed: 17339843]

Wislet-Gendebien S, Hans G, et al. Plasticity of cultured mesenchymal stem cells: switch from nestin-positive to excitable neuron-like phenotype. Stem Cells 2005;23(3):392–402. [PubMed: 15749934]

Woodbury D, Reynolds K, et al. Adult bone marrow stromal stem cells express germline, ectodermal, endodermal, and mesodermal genes prior to neurogenesis. J Neurosci Res 2002;69(6):908–17. [PubMed: 12205683]

Woodbury D, Schwarz EJ, et al. Adult rat and human bone marrow stromal cells differentiate into neurons. J Neurosci Res 2000;61(4):364–70. [PubMed: 10931522]

Yang LY, Liu XM, et al. Adipose tissue-derived stromal cells express neuronal phenotypes. Chin Med J (Engl) 2004;117(3):425–9. [PubMed: 15043785]

Yasuhara T, Matsukawa N, et al. Transplantation of human neural stem cells exerts neuroprotection in a rat model of Parkinson's disease. J Neurosci 2006;26(48):12497–511. [PubMed: 17135412]

Ye M, Chen S, et al. Glial cell line-derived neurotrophic factor in bone marrow stromal cells of rat. Neuroreport 2005;16(6):581–4. [PubMed: 15812312]

Ye M, Wang XJ, et al. Transplantation of bone marrow stromal cells containing the neurturin gene in rat model of Parkinson's disease. Brain Res 2007;1142:206–16. [PubMed: 17336273]

Zuk PA, Zhu M, et al. Human adipose tissue is a source of multipotent stem cells. Mol Biol Cell 2002;13 (12):4279–95. [PubMed: 12475952]

Zuk PA, Zhu M, et al. Multilineage cells from human adipose tissue: implications for cell-based therapies. Tissue Eng 2001;7(2):211–28. [PubMed: 11304456]

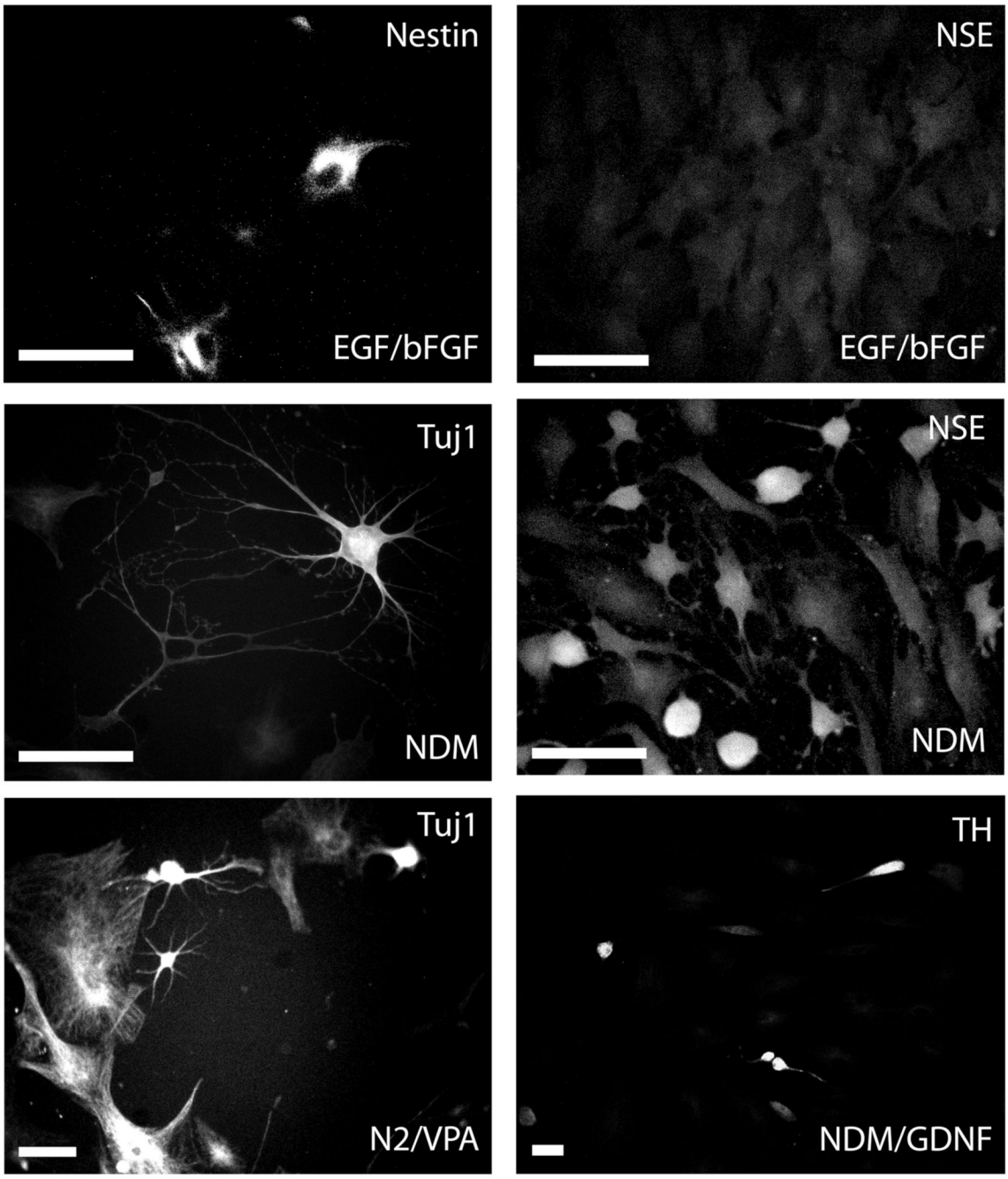

Figure 1. Immunocytochemical analyses of cellular marker expression in naïve and differentiated rat ADAS cells

Representative examples of passage 3 naïve and differentiated ADAS cells immunostained for specific neural cell markers (See Materials and Methods). Treatments were as follows: EGF/FGF-2 for 2 days; NDM: 2 days in EGF/FGF-2 plus 4 days in NDM; N2/VPA: 2 days in EGF/FGF-2 plus 4 days in N2 supplement + 0.5mM VPA; 10ng/mL GDNF. Data shown are representative of six independent experiments. Scale bar = 50 um.

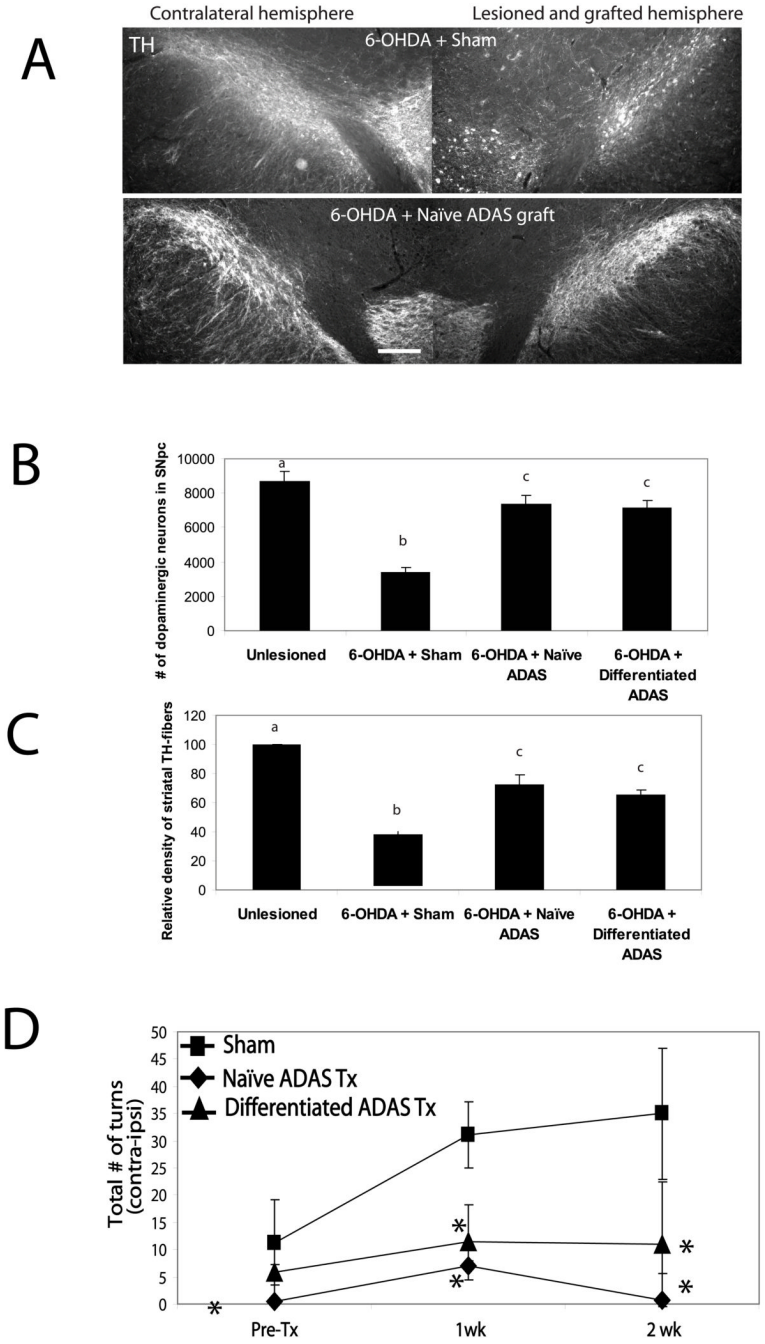

Figure 2. ADAS cell transplants attenuated loss of nigral and striatal tyrosine hydroxylase immunoreactivity and rotational behavior in 6-OHDA lesioned rats

Comparison of midbrain dopaminergic (tyrosine hydroxylase-positive) cell bodies and fiber immunoreactivity at 4 weeks post-lesion in control (unlesioned, n = 4), 6-OHDA-lesioned (n = 4), 6-OHDA-lesioned with sham (n = 4) transplant, 6-OHDA-lesioned with passage 2 naïve ADAS cells transplant (n = 5), or passage 2 differentiated ADAS cells transplant (n = 5). A, Representative rostral midbrain sections from 6-OHDA/Sham and 6-OHDA/naïve ADAS transplanted rats were stained with an antibody against tyrosine hydroxylase (TH). The 6-OHDA-lesioned hemisphere in the sham-transplanted rat displayed significant loss of TH-immunoreactivity in SNpc relative to the contralateral (unlesioned) side whereas 6-OHDA-

lesioned hemisphere of rat that also received a naïve ADAS cell transplant displayed significant sparing of TH-positive cell bodies and fibers. Scale bar = 400 um. B, Stereological estimates of nigral DA neuron number, and C, Relative density of striatal TH-positive fibers confirm the neuroprotective effects of the autologous grafts of naïve and differentiated ADAS cells against 6-OHDA-induced loss of nigral TH-positive dopaminergic neurons (see Materials and Methods). Values expressed for neuron number and striatal density are group means ± S.D. Values were compared by one-way ANOVA followed by Tukey-Kramer HSD post-hoc test. Groups with different letters are significantly different at $p<0.05$. D, Rotational behavior was monitored for 20 minutes after amphetamine administration at 2.5 mg/kg i.p. (see Materials and Methods) as an indirect measure of striatal dopamine depletion induced by 6-OHDA. 6-OHDA-lesioned rats that received passage 2 naïve ADAS cells (black diamonds, n = 5) or NDM-treated ADAS cells (black triangles, n = 5) displayed attenuated amphetamine-induced rotational behavior compared to 6-OHDA-lesioned sham-transplanted (black squares, n = 4) rats. Values expressed are the group means ± S.D. Values were compared by one-way ANOVA followed by Tukey-Kramer HSD post-hoc test. Groups marked with an asterisk (*) are significantly different from sham at $p < 0.05$.

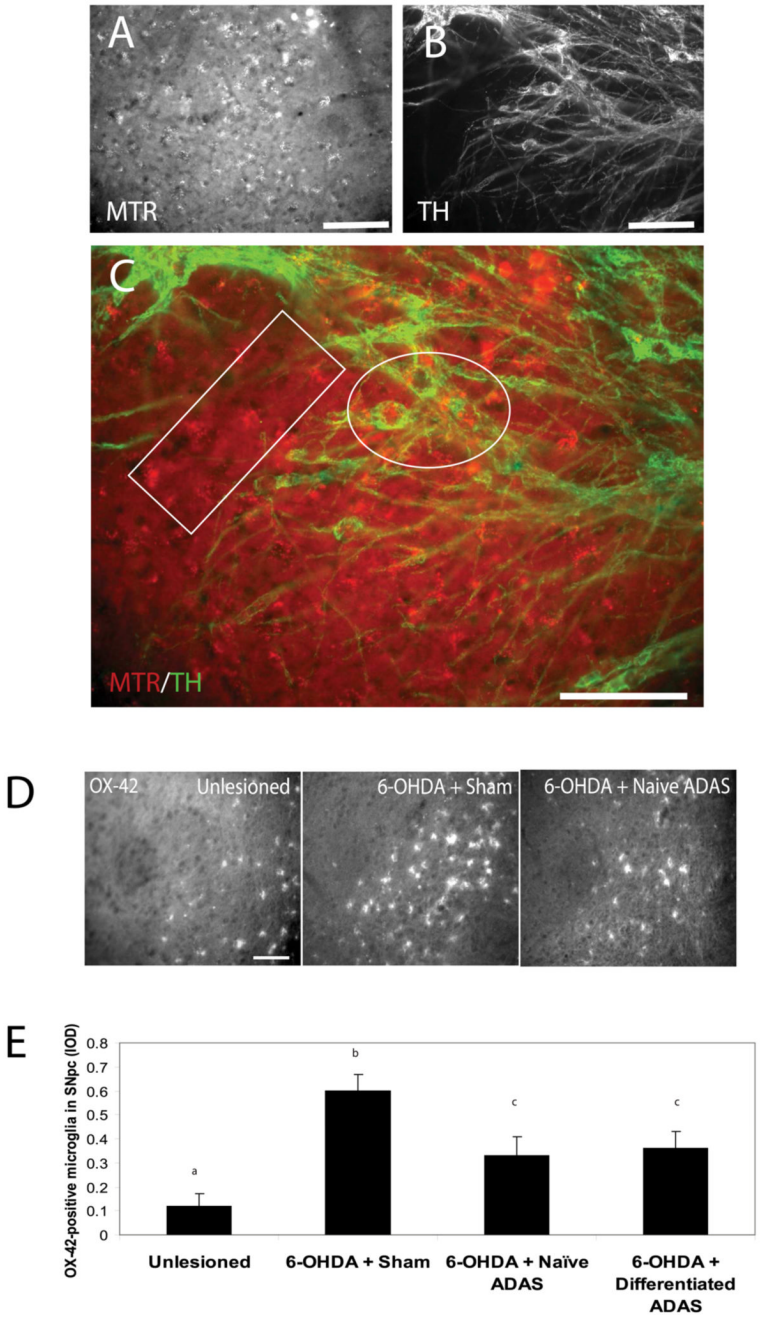

Figure 3. Transplanted ADAS cells engraft in 6-OHDA lesioned brains and attenuate microglial activation

A, Mitotracker labeled ADAS cells in midbrain sections of rats lesioned with the oxidative neurotoxin 6-hyroxydopamine (see Materials and Methods). B, Expression of the dopaminergic marker TH is not detectable in ADAS cells after transplantation. C, In merged images, the white box indicates a region with singly labeled (MTR-positive) ADAS cells and the white oval indicates a region where MTR-labeled ADAS cells (red) were in close proximity to TH-positive (green) neuron cell bodies. D, Representative images of OX-42-positive microglial staining in SNpc of unlesioned, 6-OHDA-lesioned/sham-transplanted, and 6-OHDA-lesioned naïve ADAS cell-transplanted animals reveal attenuation of

neuroinflammatory response in animals that received the ADAS cell transplants compared to lesioned animals that received a sham-transplant. E, Quantification of microglial burden in SNpc, IOD = integrated optical density (see Materials and Methods). Values are means ± S.E.M. Values were compared by one-way ANOVA followed by Tukey-Kramer HSD post-hoc test. Groups with different letters are significantly different at $p<0.05$. Scale bars=200 um.

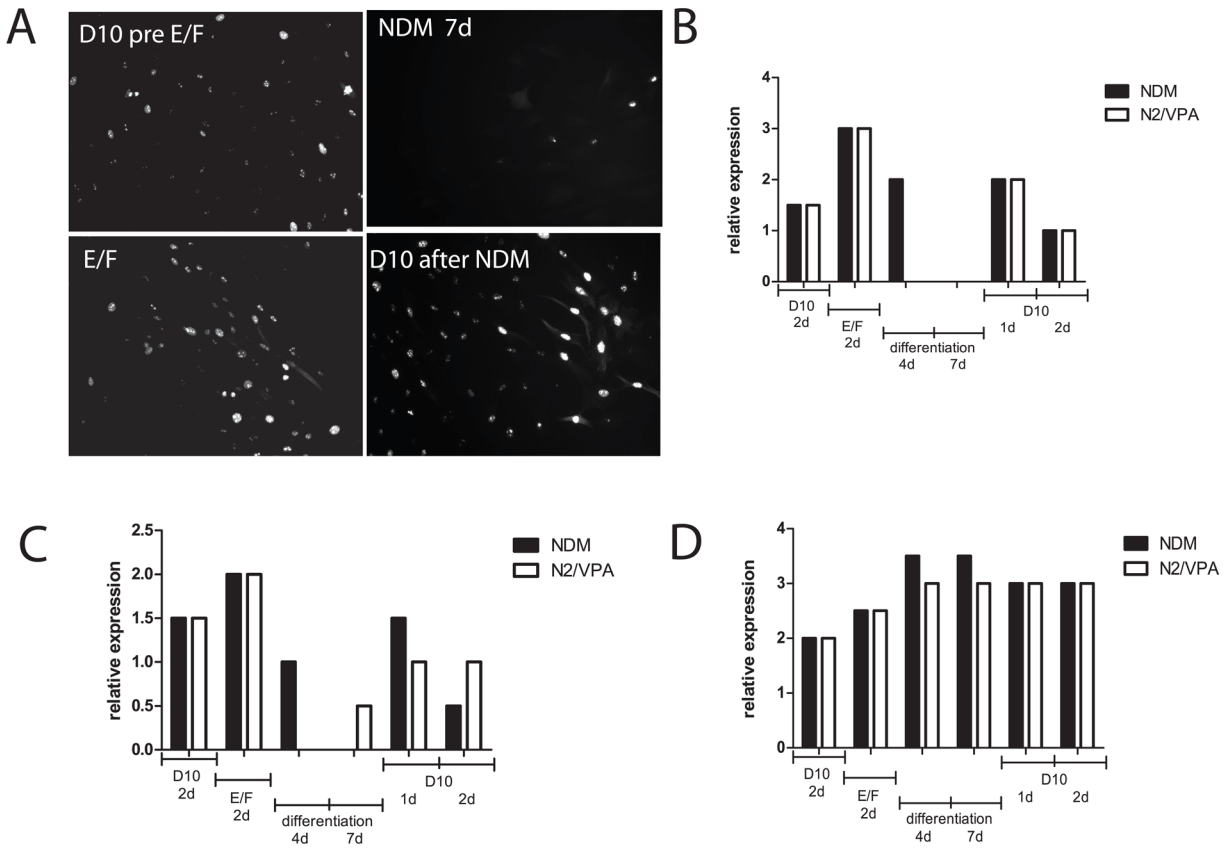

Figure 4. Stability of differentiated phenotypes of ADAS cells *in vitro*

A survey of immunoreactivity for each protein marker was performed after the indicated treatment conditions leading up to, during, and following differentiation with NDM (black bars) or N2/VPA exposure (white bars) at high (40x objective) and low (10x objective) magnification. Scores between 1 and 4 were assigned by investigators blinded to the treatment based on fluorescence intensity and fraction of total cells expressing that particular marker according to the following scale: 4 = intense immunoreactivity in many (> 50 %) of the cells, 3 = strong staining in approximately 50% of the cells, 2 = detectable staining in less than 50% of the cells, 1 = detectable staining in a small fraction (< 10%) of the cells, 0 = no detectable immunoreactivity (Panels B, C, D). Independent of which differentiation medium was used (NDM (black bars) or N2/VPA (white bars), See Materials and Methods), results were similar for each of the different markers. A, Nuclear proliferation antigen Ki-67 expression (immunofluorescence) in ADAS cells under the conditions indicated. B, Relative expression of Ki-67 in ADAS cell culture under the conditions indicated, C, Relative expression of nestin in ADAS cell culture under the conditions indicated. D, Relative expression of Tuj-1 in ADAS cell culture under the conditions indicated. Data shown are representative of two independent experiments.

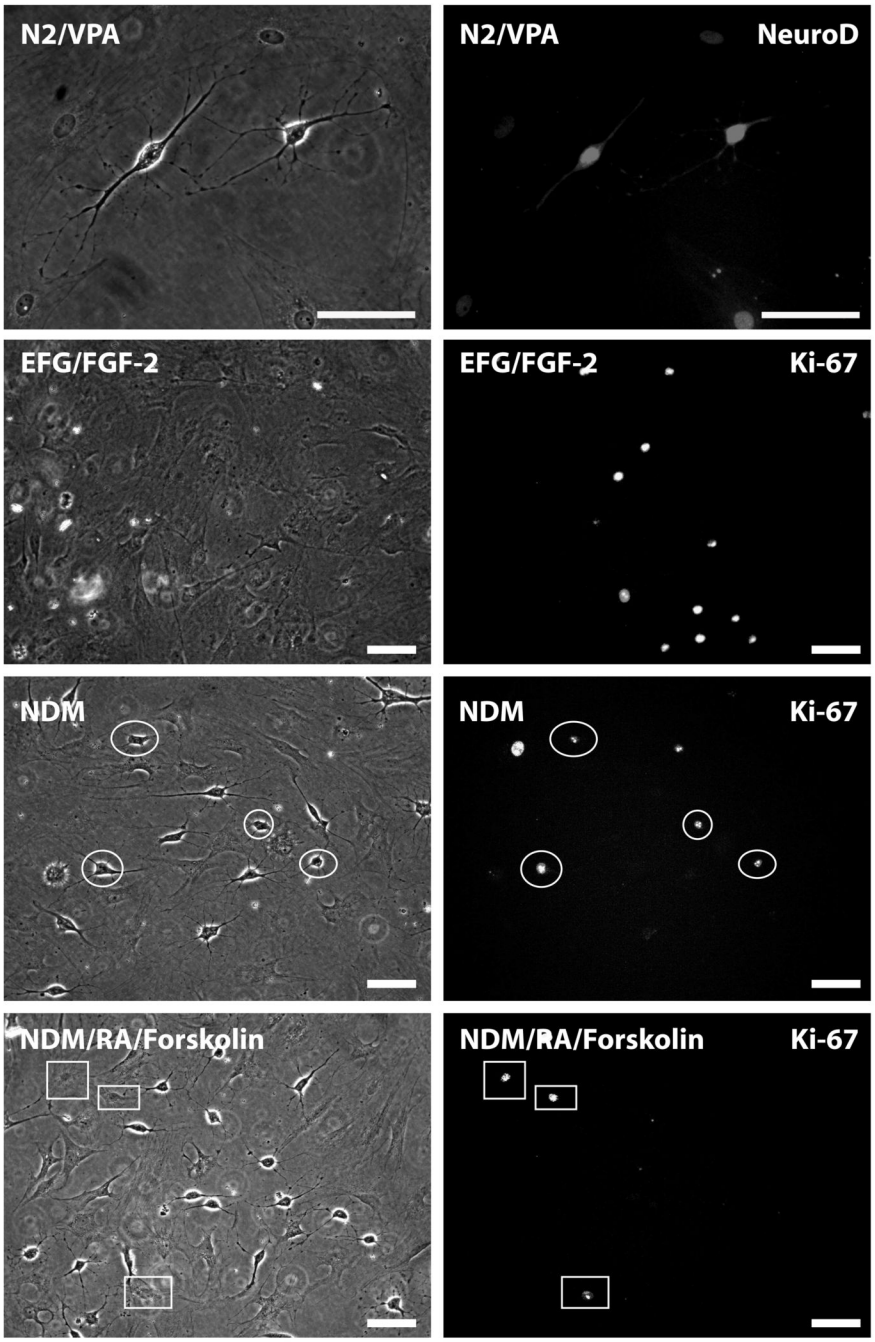

Figure 5. Cell cycle arrest and terminal differentiation of morphologically differentiated ADAS cells requires exposure to retinoid acid and forskolin

N2/VPA-treated ADAS cell cultures (passage 3) were immunostained with an antibody against NeuroD. Persistent expression of Neuro D was detectable in both undifferentiated (flatter) and in morphologically differentiated ADAS cells. Expression of nuclear proliferation antigen Ki-67 was detectable in subpopulations of ADAS cells growing in EGF/FGF-2 and in some morphologically differentiated ADAS cells exposed to NDM (white ovals). Cell cycle arrest was achieved in morphologically differentiated cells only after supplementation of NDM with RA and forskolin, as evidenced by presence of Ki67 only in non-differentiated cells (white rectangles). Treatments were as follows: EGF/FGF-2 2 days, NDM: 2 days EGF/FGF-2 plus

4 days NDM; N2/VPA: 2 days EGF/FGF-2 plus 2 days N2/VPA; NDM/RA/Forskolin: 2 days EGF/FGF-2 plus 4 days NDM + 1uM RA/10uM Forskolin. Data shown are representative of three independent experiments. Scale bar = 50 um.

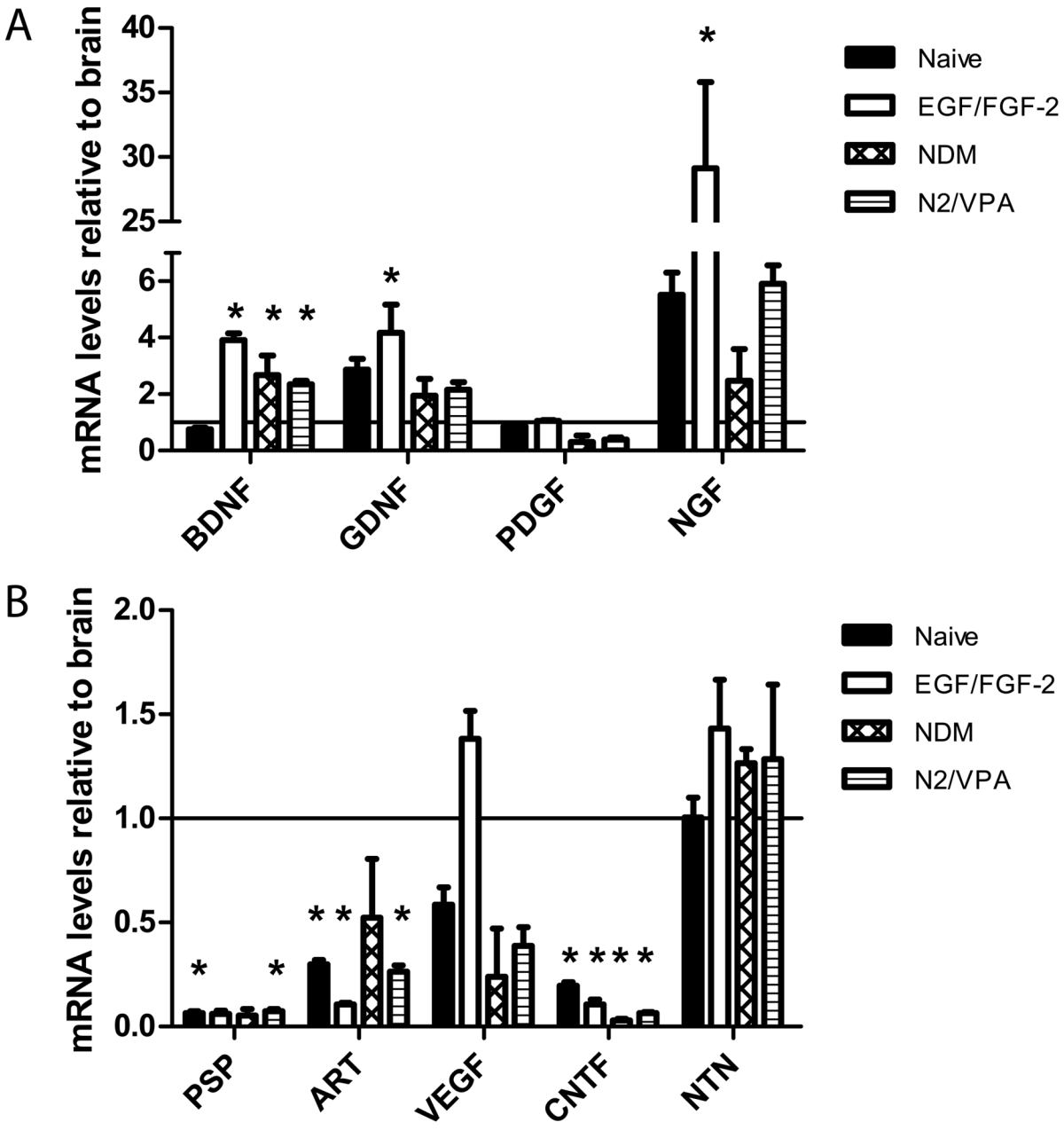

Figure 6. ADAS cells express potent dopaminergic survival factors *in vitro*

To investigate the growth factor expression profile of the cells relative to total brain levels just prior to transplanatation, ADAS cells were plated and treated as follows at passage 2 or 3 prior to harvesting for real-time quantitative PCR analysis or in the case of neurturin, for semi-quantitave RT-PCR analysis (see Materials and Methods). A, Expression of BDNF, GDNF, and NGF by ADAS was found to be higher than brain levels. B, Expression of NTN and VEGF by ADAS was found to be equivalent to that in total brain; while expression of ART and CNTF was below that of total brain and PSP was undetectable. Cells were grown in D10, grown in D10 then proliferated for 2 days in D10 supplemented with 10ng/mL EGF and 20ng/mL FGF-2, or grown in D10, proliferated in EGF/FGF-2, and exposed to NDM or N2/VPA for 2 days. Differences in expression of mRNAs between rat brain and ADAS cultures were analyzed by

single factor ANOVA followed by Tukey's post hoc test (GraphPad). Values expressed are means +/− SEM normalized to rat brain (indicated by a solid horizontal line). Genes with asterisks (*) are significantly different from brain at the level of $p<0.05$). Each condition was plated in triplicate. Differences between each group and whole brain were analyzed by single factor ANOVA followed by Tukey's HSD post-hoc test (GraphPad). Values expressed are mean mRNA levels relative to brain levels +/− SEM. Bars marked with an asterisk (*) significant at the level $p < 0.05$).

Table 1

Summary of Immunocytochemical analyses of cell marker expression in naive (undifferentiated) and differentiated ADAS cells

Markers	D10 Medium	D10→ EGF/FGF-2 2d	D10→ EGF/FGF-2→ NDM 4d	D10→ EGF/FGF-2→ N2/VPA 4d	NSA Prolif→ NSA Differentiation 4d
Fibronectin	+++	+++	++	++	++
Vimentin	+	++	++	+	++
Nestin*	+	++	+	+	+
VE Cadherin*	−	+	++	++	+
Neuro D*	−	+/−	++	+++	+
Tuj1*	−	+/−	++	++	++
NSE*	−	−	++	++	++
NeuN	−	−	+/−	+/−	++
MAP2b	−	−	+/−	+/−	++
GABA	−	−	+	+/−	+/−
ChAT*	−	−	+/−	+/−	+/−
TH*	−	−	+/−	+/−	+/−
GFAP*	−	+	+/−	+/−	+
S100β*	−	+/−	+/−	+/−	+/−
O4	−	+/−	+/−	+/−	+/−
SMA*	++	++	+/−	+/−	++
TrkB	−	−	+	+	+
OX-42	−	+/−	−	−	−
p75NTR	−	+/−	−	−	+/−
MBP	−	−	−	−	−

* denotes that mRNA confirmed by real time QPCR. Studies were performed on ADAS cells at passages 2 through 4.

+++ = robust expression in >50% of the cells

++ = strong expression in ~ 50% of the cells

+ = detectable expression in < 50% of the cells

+/− = detectable expression in small percentage (<10%) of the cells

− = no detectable expression